



Enhanced performance of quantum cascade Raman laser



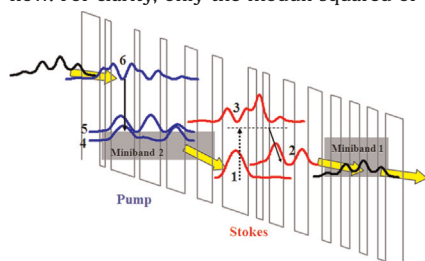
Hossein Reza Yousefvand ^{a,*}, Vahid Aahmadi ^b

^a Department of Electrical Engineering, Islamshahr Branch, Islamic Azad University, Islamshahr 33147-67653, Iran

^b Department of Electrical and computer Engineering, Tarbiat Modares University, Tehran 14115-194, Iran

GRAPHICAL ABSTRACT

The design and modeling of a quantum cascade Raman laser based on monolithic integration of stimulated Raman scattering and pump source. This potential-energy profile of the conduction band illustrates the monolithic integration concept of the quantum cascade Raman laser. Energy levels involved in stimulated emission (levels 6, 5 and 4), which serves as a pump laser, are shown, as well as the energy levels required for stimulated Raman scattering (levels 1, 2 and 3), which absorbs pump photons and emits photons as longer wavelength. The yellow arrows indicate the direction of electron flow. For clarity, only the moduli squared of the most important wave functions are shown.



ARTICLE INFO

Article history:

Received 10 November 2014

Accepted 29 January 2015

Available online 30 January 2015

Keywords:

Quantum cascade lasers
Stimulated Raman scattering
Nonlinear effects
Rate equations

ABSTRACT

We present a self-consistent numerical approach for quantum cascade Raman laser (QC-RL) with a modified design to improve the device performance. Our modeling approach is based on monolithic integration of stimulated Raman scattering (SRS) and electrically pumped QC laser. The laser band structure utilizing techniques with both material-dependent effective mass and band nonparabolicity is calculated by solving the Schrodinger–Poisson equations self-consistently. A detailed analysis of output characteristics of the obtained structure is carried out within a simplified 4-level rate equations model taking into account the SRS process. The model accurately explains the operating characteristics found in QCLs, such as damping transient response and non-resonant behavior of modulation frequency response. Furthermore, modification of the structure is focused on improving the SRS in the QC-RL. This leads to an enhancement of the device performance such as threshold current, external quantum efficiency, conversion efficiency, turn-on delay and modulation response. The excellent agreement of the experimental data with the simulated light output-current characteristics confirms the validity of the model.

© 2015 Elsevier B.V. All rights reserved.

1. Introduction

Quantum cascade lasers (QCLs) [1] are unipolar semiconductor devices based on optical and electronic transitions between

quantized states in multiple quantum well structures. The active material of a QCL typically contains a cascade of many, often several 10, pairs of active regions and injectors. The cascading scheme and unipolarity are two characteristic features of QCLs that make this kind of device so unique. It is also possible to selectively replace active regions and/or injectors with other optical elements such as active regions of another wavelength, which leads to multiple wavelength emission, or nonlinear optical elements [2,3].

* Corresponding author.

E-mail addresses: hossein@iaau.ac.ir (H.R. Yousefvand),
v_aahmadi@modares.ac.ir (V. Aahmadi).

Nonlinear light generation in QCLs has the potential to extend the operating wavelength of these devices outside the limits imposed by the fundamental properties of the materials of choice. With the advent of powerful QCL at selected frequencies, it has now become possible to generate new frequencies by stimulating Raman scattered waves of these light sources. The Raman scattering effect is the inelastic scattering [4] of a photon with an optical phonon, which originates from a finite response time of the third order nonlinear polarization of the material [5]. When a pump field propagates in a medium (laser cavity), spontaneous Raman scattering occurs. It transfers some of the pump photons to new frequencies (Raman photons). For strong pump fields the number of emitted Raman photons is high, and they can stimulate further (coherence) Raman photons to be emitted in the direction of the pump beam. This process is known as stimulated Raman scattering (SRS). To date, Stokes and Anti-Stokes Raman lasing in QCLs has been achieved in different separate theoretical and experiment works [6–9]. The device structure studied in this paper is based on a mid-infrared Raman injection laser which emits at two wavelengths [7] (6.7 μm of the pump and 8.9 μm for Stokes).

To investigate and understand the physical processes of SRS in QCLs, comprehensive and self-consistent theoretical modeling approach is required. In this work, in order to improve the agreement of our model calculations with experimental results we develop the theoretical model of our previous work [9]. The band structure of the laser is calculated by solving the coupled Schrodinger–Poisson equations self-consistently. Based on scattering models [10–13], the electron dynamics between the various regions of the structure described by a 18-level system simplified to a 4-level rate-equation model. This paper is focused on improving the performance of QC-RL by proper design of the electronic level structure. By including important additional effects; we proposed an improved pump/Stokes design with enhanced Stokes Raman nonlinearity. Compared to reference structure, which is based on a two-phonon resonance design, the pump region of modified structure is based on three-phonon resonance depopulation scheme, which provides the faster intersubband relaxation process [14].

2. Model and theory

2.1. The QC-RL structure

We begin with the initial structure of QC-RL reported in [7], which is a InP-based lattice matched InGaAs–InAlAs designed for SRS. In the QC-RL, all active sections contain an injector, a pump region, a Stokes region and a collector, which is equal to $1/3$ periods of the full cascade in the structure. In order to calculate the band structure of QC-RL, the built-in electric potential is discretized with the spatial interval of 1 Å. The Schrodinger and Poisson equations with the material dependence effective mass and band non-parabolicity are solved numerically by the finite difference method [15,16]. The effective band profile including the built-in potential and the electric field generated by positively ionized donor and negatively charge electrons is calculated by iteratively solving the Schrodinger and Poisson equations until the electronic structure converges. Additionally, the energy levels and associated wavefunctions involved in all portions of the structure, which then used to evaluate the electron–longitudinal optical (LO) phonon scattering rates, are obtained. Fig. 1 gives the calculated band profile and squared amplitude of the wavefunctions involved in the $1/3$ periods of the structure under an electric field of 50 kV/cm. The major inelastic scattering mechanism in InGaAs/InAlAs systems is via the electron–LO-phonon interaction [17], and we take into account only this process based on Ferreira and Bastard’s approach [18]. In order to evaluate the relevant dipole matrix element calculation, we adopted

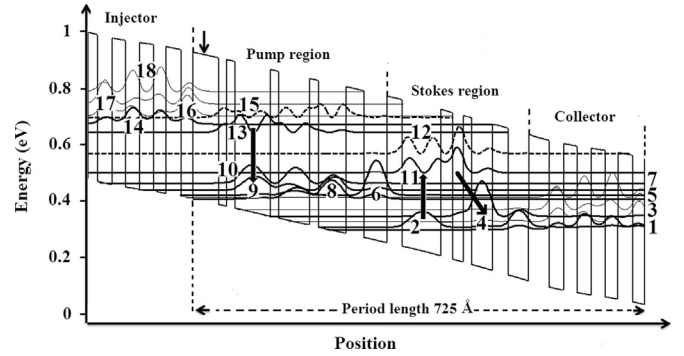


Fig. 1. Schematic conduction band diagram and squared amplitude of the wavefunctions involved in the $1/3$ periods of QC-RL laser with the self-consistent calculation. The layer thicknesses (in Å) for one stage of laser from left to right starting from the barrier indicated by an arrow are: **42/13/14/56/14/49/15/43/30/36/25/61/20/16/15/32/26/32/34/22/23/21/24/19/25/18**. In_{0.52}Al_{0.48}As-barrier layers are in bold, and In_{0.53}Ga_{0.47}As-well layers are in regular, and doped layers ($n = 4 \times 10^{17} \text{ cm}^{-3}$) are underlined.

the formulation described in [19], in which we consider the influence of the valence band part of the wavefunctions.

As shown in Fig. 1 energy diagram of the QC-RL consists of eighteen-level. Each of injector and collector regions is presented by four energy levels, i.e., subbands 1, 3, 5 and 7 for collector and subbands 14, 16, 17 and 18 for injector. Radiative transitions occur between levels 13 and 10 in the pump region, while upper lasing level 13 is populated by injection of electrons from the four levels of injector. In order to fast extraction of electrons from the lower lasing state, the levels 10, 9 and 8 are equally spaced, and the energy intervals are near to an LO-phonon energy. The pump laser provides high optical power density and, at the same time, relaxed electrons of the lower lasing state tunnel through barrier into the Stokes region. Therefore, electrons in level 2 of the Stokes region undergo Stokes–Raman scattering stimulated by the pump light (with $\hbar\omega_p$ energy) emitting photons with $\hbar\omega_s$ energy (corresponding to 11 \rightarrow 4 energy transition), called Stokes radiation.

2.2. Carrier dynamics

In order to facilitate system-level design and output characteristic simulation, we assume two reasonable approximations about the carrier dynamics in the structure. The first, we assume that carriers are sufficiently quickly and exclusively injected into the upper lasing state (level 13) from the injector’s ground state (level 14), and can exit from the lower lasing state of the pump region (levels 10) into the following Stokes state (level 2). The second, by neglecting population of non-lasing states, a 18-level self-consistent rate equations is simplified to a 4-level of rate-equation model (corresponding to levels 13, 10, 4 and 2). Considering a unity injection efficiency, the system of rate equations for electron population n_{13} and n_{10} in levels 13 and 10, and the evolutions of photon population n_p in the pump region expressed as [20]

$$\frac{dn_{13}}{dt} = \frac{I}{e} - \frac{n_{13}}{\tau_{13}} - \Gamma_p \frac{c' \alpha_{13,10}}{V} (n_{13} - n_{10}) n_p \quad (1)$$

$$\frac{dn_{10}}{dt} = \frac{n_{13}}{\tau_{13,10}} - \frac{n_{10}}{\tau_{10eff}} + \Gamma_p \frac{c' \sigma_{13,10}}{V} (n_{13} - n_{10}) n_p \quad (2)$$

$$\frac{dn_p}{dt} = N_m \frac{c' \sigma_{13,10}}{V} (n_{13} - n_{10}) n_p - \frac{n_p}{\tau_p} \quad (3)$$

where e is the electronic charge, I is the electron injection current tunneling into level 13, V is the volume of the cavity, N_m is the

Download English Version:

<https://daneshyari.com/en/article/1544205>

Download Persian Version:

<https://daneshyari.com/article/1544205>

[Daneshyari.com](https://daneshyari.com)